Welding of thermoplastics by means of carbon-nanotube web

Russello, M., Catalanotti, G., Hawkins, S. C., & Falzon, B. G. (2020). Welding of thermoplastics by means of carbon-nanotube web. *Composites Communications*, *17*, 56-60. https://doi.org/10.1016/j.coco.2019.11.001

Published in:
Composites Communications

Document Version:
Peer reviewed version

Journal Pre-proof

Welding of thermoplastics by means of carbon-nanotube web

M. Russello, G. Catalanotti, S.C. Hawkins, B.G. Falzon

PII: S2452-2139(19)30158-5

DOI: https://doi.org/10.1016/j.coco.2019.11.001

Reference: COCO 270

To appear in: *Composites Communications*

Received Date: 23 July 2019

Revised Date: 4 October 2019

Accepted Date: 1 November 2019

Please cite this article as: M. Russello, G. Catalanotti, S.C. Hawkins, B.G. Falzon, Welding of thermoplastics by means of carbon-nanotube web, *Composites Communications*, https://doi.org/10.1016/j.coco.2019.11.001.

Welding of thermoplastics by means of carbon-nanotube web

M. Russello[1], G. Catalanotti[1*], S.C. Hawkins[1,2], B.G. Falzon[1†]

1. Advanced Composites Research Group (ACRG), School of Mechanical and Aerospace Engineering, Queen's University Belfast, Belfast BT9 5AH, UK

2. Department of Materials Science and Engineering, Monash University, Clayton 3800, Australia

Abstract

We report the welding of thermoplastic materials by means of embedded fully-aligned carbon nanotube (CNT) web. Layers of CNT web (each layer of which has a densified thickness of 50 nm) were placed between two polyether ether ketone (PEEK) films to create a resilient insert which was then embedded between two bonding interfaces. An electrical current was passed through the CNT webs to activate Joule heating, melting the insert and adjacent surfaces of the thermoplastic parts. Preliminary experiments on welded PEEK samples show that the tensile strength of the welded specimens reached 96% of the strength of the pristine material, even before optimizing the processing conditions. The potential of this welding technology is evident: the inserts are ultra-thin, highly flexible, so can conform to bonding surfaces of complex shape, and the anisotropy of the CNT-web provides an additional variable for optimizing the electro-thermal response.

Keywords: Thermoplastics, Carbon-nanotube (CNT) webs, Resistance welding, Fusion bonding

[*] Corresponding author. Tel.: +44 (0)28 9097 4502.
E-mail address: g.catalanotti@qub.ac.uk
[†] Corresponding author. Tel.: +44 (0)28 9097 5640.
E-mail address: b.falzon@qub.ac.uk

1. Introduction

Fusion bonding is a well-established method for welding thermoplastics [1–7] which entails the controlled melting of the mating surfaces and their consolidation under applied pressure. Fusion-bonding techniques may be classified according to the heat generation mechanism into: (i) mechanical welding; (ii) thermal welding; and (iii) electromagnetic welding [7]. Electromagnetic welding, in turn, may be subdivided into induction welding, microwave welding and resistance welding depending on whether the heating produced in the conductive material placed at the bonding surface is generated through an induction coil, microwave radiation, or by the direct application of an electric potential.

Resistance welding is a simple, low-cost joining solution for thermoplastic materials but generally requires a metal mesh or carbon fibre insert as the heating element [6,8–10] which remains in the joint after welding. Metal inserts may have a detrimental effect on the mechanical performance of the joint [11]), add to the weight of the assembly and be susceptible to corrosion. Carbon fibres are light and resistant to corrosion, but they are stiff and difficult to introduce at geometrically complex interfaces. Moreover, they may also cause a reduction in mechanical properties and poor weld reproducibility, especially when a large quantity of fibre is used. Electrical connections between the electrodes and the carbon fibres are also problematic. Such factors hinder the process of scaling up the technology [12]. Brassard et al. [13] proposed a new heating element made of polyetherimide (PEI) made electrically conductive by mixing dispersed multi-wall carbon nanotubes (MWCNT). It is known that the dispersion of CNTs inside a polymer matrix is not easy, especially when viscous polymers are employed. Moreover, the dispersed CNTs, which are randomly oriented, create isotropic thermal behaviour and thus obstruct the fabrication of a specific heating path.

An innovative solution [14] is demonstrated that uses highly-aligned carbon nanotube web (CNT-web) as a directly energised resistive heating element, which could potentially overcome the aforementioned shortcomings. CNT webs are ~10^4 times lighter than carbon fibres of similar

resistance and a single layer of CNT-web has a densified thickness of only around 50 nm, so the inclusion effect is mitigated, if not eliminated. CNT-web is essentially catalyst-free and not prone to corrosion; the web can be laterally collapsed to form a yarn outside the joint, thereby facilitating connection to electrodes. The webs exhibit high flexibility and conformability, allowing the welding of very complex bonding surfaces, and their anisotropy can be exploited to tailor an optimal electro-thermal response for the welding process [15,16].

2. Materials and Methods

2.1 CNT-web insert preparation and characterization

Directly drawable CNT forests, with an average CNT length of 300 μm, and an average diameter of 10 nm, were synthesized by chemical vapour deposition (CVD) following a procedure reported in [17]. CNT-web was drawn directly from the silicon growth substrate and wound to a depth of 10 layers onto a square-section mandrel (side 70 mm) lined with a 220 μm thick PEEK film (Fig. 1a). The PEEK film, bearing the CNT-web, was removed and cut into squares with sides of length 16 mm. Conductive silver paint was sprayed onto the ends of the web to create electrodes perpendicular to the drawn direction. Copper busses were then stuck to the paint to facilitate electrical connections (Fig. 1b). A second PEEK film was then placed over the assembly to create the insert.

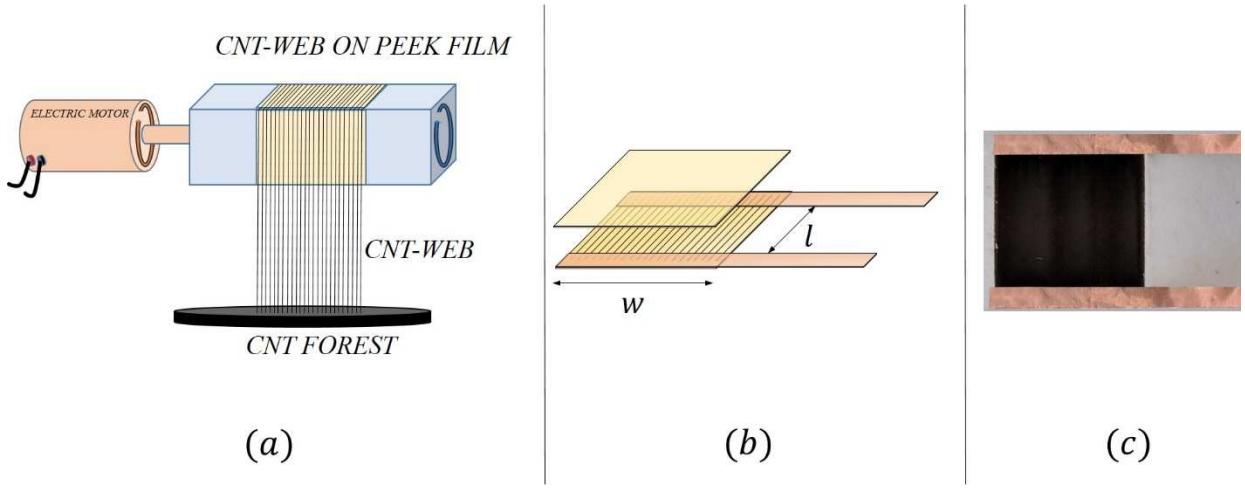

Figure 1 – Insert manufacturing. (a) Drawing and winding of carbon nanotube web, (b) assembly of the insert with copper electrodes and covering film(c) top view of the final insert before covering.

The longitudinal sheet resistivity of a single layer of CNT-web, $\rho_{sheet} = 1200 \pm 160$ Ohm. This was calculated as $\rho_{sheet} = RwN/l$, where R is the longitudinal resistance of N web layers measured with an Agilent 34450A 5½ Digit Multimeter, $N = 10$ is the number of CNT-web layers, $w = 16$ mm is the width of the specimen, and $l = 14$ mm is the inner distance between the electrodes (see Fig. 1b).

2.2 Welding process

A Platen Press (COLLIN P 200 P) was used to make PEEK panels with a thickness of 10 mm following the supplier's recommended manufacturing protocol using PEEK pellets. The panels were machined using a CNC machine (Stepcraft 600) in order to obtain samples of dimensions 10 mm × 10 mm × 130 mm for weld specimens and 10 mm ×10 mm × 260 mm for controls. Before welding, surfaces to be joined were carefully cleaned with acetone to remove any contamination.

The welding process (Fig. 2) consists of five steps:

(i) alignment of the specimens (Fig. 2a);

(ii) positioning of the insert (Fig. 2b) with slight pressure applied;

(iii) application of electric power to melt insert and adjacent regions of the specimens (Fig. 2c);

(iv) application of a consolidation pressure as heating is stopped (Fig. 2d);

(v) machining to remove the welding flash.

Alignment of the two specimens to be joined, and controlled application of pressure, was achieved with the ASTM D6641 test fixture (Fig. 2a). Heat is generated within the insert by the Joule effect and the total electrical energy used, $E = Wt$, where t is the time of exposure and the power,

$W = VI$ (i.e. applied DC voltage times current). The power is kept constant (by adjusting the voltage) for the duration of heating. It is also convenient to use specific power, W_s , and specific input energy, E_s, obtained by normalising the power and energy with respect to the area of the bonding surface. The specimens were all welded at the same specific power $Ws = 55$ kW/m^2 while the effects of consolidation pressure,p, and time as expressed by specific input energy, Es, were studied.

A thermal imaging camera and software (FLIR T640, ResearchIR) was employed to record the temperature profile during the entire process to investigate the change in the superficial temperature in the vicinity of the weld line; to understand the effects of the welding parameters on the temperature distribution; and to analyse heating and cooling rate of the samples.

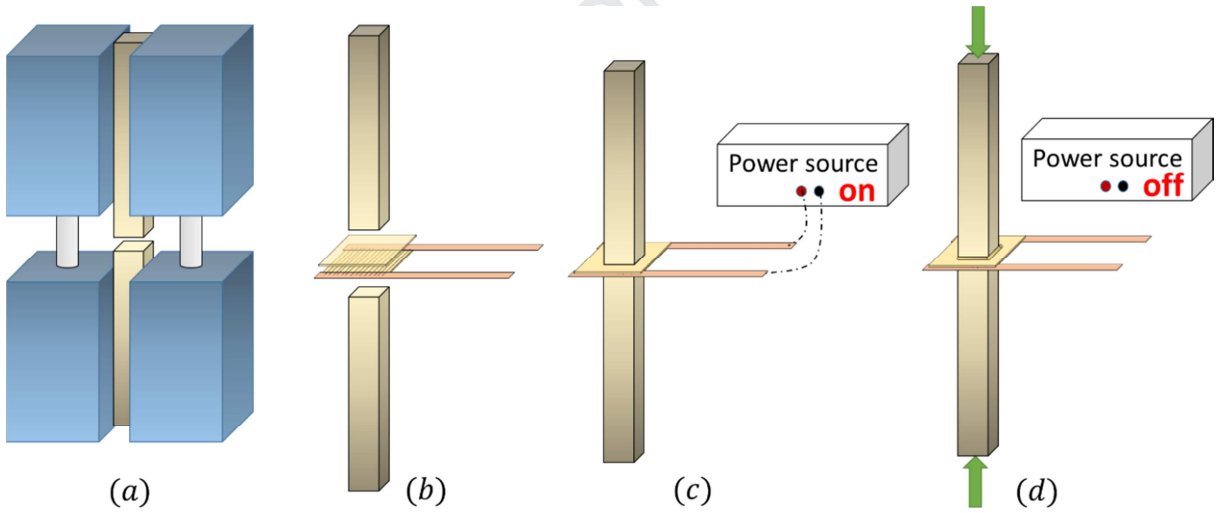

Figure 2 – Welding process. (a) Alignment of polymeric parts with ASTM D6641 – combined loading compression test fixture, (b)positioning of CNT-web insert, (c) application of electric power, and (d) application of consolidation pressure (b-d, ASTM D6641 fixture deleted for clarity)

2.3 Characterization

2.3.1 Mechanical test

Tensile tests on welded and control (pristine material) specimens were conducted using a Zwick Roell z100 universal testing machine, equipped with a 100 kN load cell, at a cross-head speed of 1 mm/min. The pristine material strength, σ_u, and that of the welded specimens, σ_w, were measured to yield a value of the joint efficiency, $e = \sigma_w/\sigma_u$.

2.3.2 Scanning electron microscope (SEM) and visual inspection

Small sections were cut across the weld line from coupons, polished, sputtered with a thin layer of gold (Agar sputter coater B7341, 30 mA for 40 s) and examined by scanning electron microscope (Hitachi FlexSEM 1000). The fractured surfaces of the specimens were also visually inspected.

3. Results and Discussion

Preliminary experiments indicated that a suitable range of pressure and input energy to explore initially was approximately 1 – 4 MPa and 5000 – 10000 kJ/m^2. Actual values and the number of specimens for each designation were selected (Table 1) to identify the best performance to-date and the effect of lower pressure and shorter time (lower input energy).

Table 1 Variables studied

Specimen Designation	Pressure, p, [MPa]	Input energy, E_s, [kJ/m2]	Specimens, #
PC Pristine Control	-	-	3
WB Weld best	4	8250	5
LP Low Pressure weld	0.4	8250	5
LE Low Energy weld	4	4950	4

The PEEK specimens to be joined were clamped with a CNT web insert between them (Fig 3a, one WB specimen ($Es = 8250$ kJ/m^2, $p = 4$ MPa) illustrated) and power applied to the copper buses.

Infrared imaging of the joint zone (Fig 3b) was captured at equilibrium temperature (about 100 seconds) and the joint held in place until cool (Fig 3c). Surface spot temperatures were continuously recorded at 0.5, 2.5, 3.5, and 5 mm (Fig 3d), respectively from the joint line where indicated (Fig 3b).

At 0.5 mm from the nominal welding line, surface temperature reaches 390 °C after about 100 seconds. It then appears to fall slightly although this is likely due to accumulation of flashing which blocks the IR camera view and presents a larger surface area for heat dissipation. Further from the joint, the temperature stabilises from about 100 seconds and then rises very slowly thereafter, reaching about 265, 200 and 155 °C, at 2.5, 3.5 and 5 mm respectively when heating is stopped (t=150 s). Thereafter, the passive cooling rate is equal to 550, 90, 35, and 20 °C/min at 0.5, 2.5, 3.5, and 5 mm, respectively.

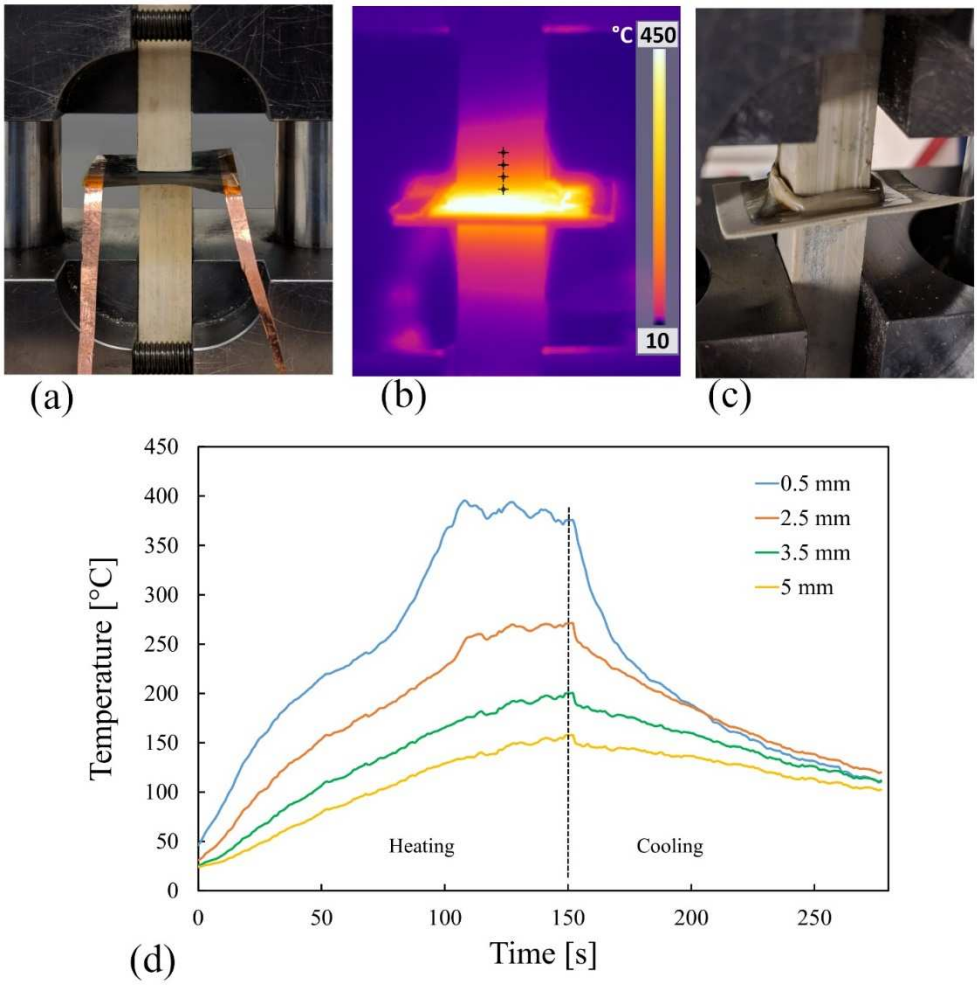

Figure 3 – (a) Setup of welding; (b)Thermal image of the WB specimen during welding; (c) welded specimen with surrounding polymer flash; (d) temperature curves at different distances from the weld line during the welding process

After cooling, the welded specimens were machined back to a 10 mm square section to remove flashing and tensile tested. Other specimens (*WB* and *LE*) were polished and analysed using the SEM. The weld region for the *WB* specimen (Fig 4a) does not show any imperfection or visible voids. Moreover, a notch was introduced in a corner of the specimen in proximity of the weld line in order to reveal the carbon nanotube location which is otherwise extremely difficult to see (detail in Fig 4a).

In contrast, the *LE* specimen exhibits a clear separation between the different regions of the joint (Fig. 4b) showing that enough energy has not been provided for melting.

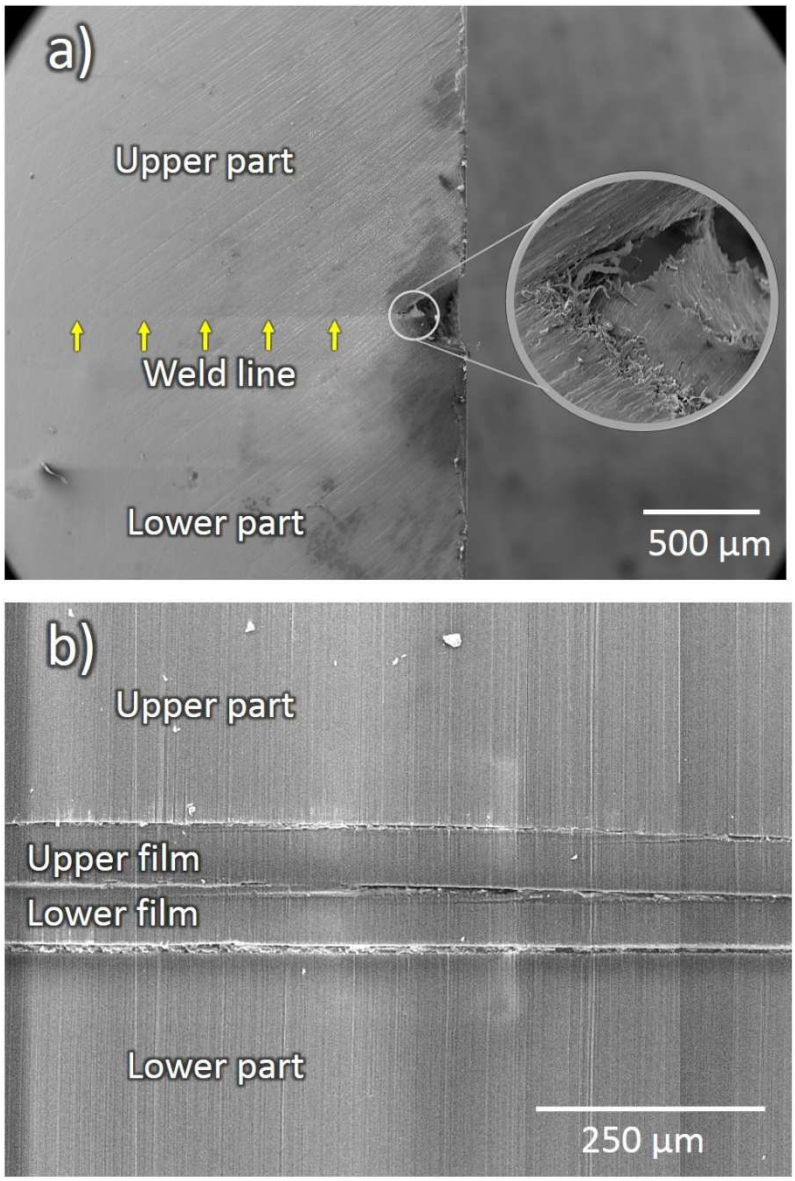

Figure 4 – SEM images of (a) WB specimen weld line with detail (mag. x10) showing the presence of CNTs, and (b) LE specimen weld line.

3.1 Mechanical performance and inspection

Mechanical testing of the welded specimens (Table 2) demonstrated that within the range of parameters studied, the best identified conditions (specimens WB) were $p = 4$ MPa and $Es = 8250$ kJ/m^2, where this total energy is delivered over a treatment period of 150 seconds.

Table 2 – Experimental results.

Designation	Tensile strength σ, [MPa]	Mean value $\bar{\sigma}$, [MPa]	SD s, [MPa]	Efficiency e, [%]

PC	102 93 103	99	6	-
WB	94 93 99 97 93	95	3	96
LP	37 7 21 12 51	25	18	25
LE	16 16 27 11	18	7	18

The simultaneous use of higher input energy and consolidation pressure (Fig. 5, Table 2) yields a bond strength of 96% efficiency. A lower pressure, and particularly a lower energy (which entails a treatment period of just 90 s) results in very poor bonding with an efficiency of just 25% and 18% respectively.

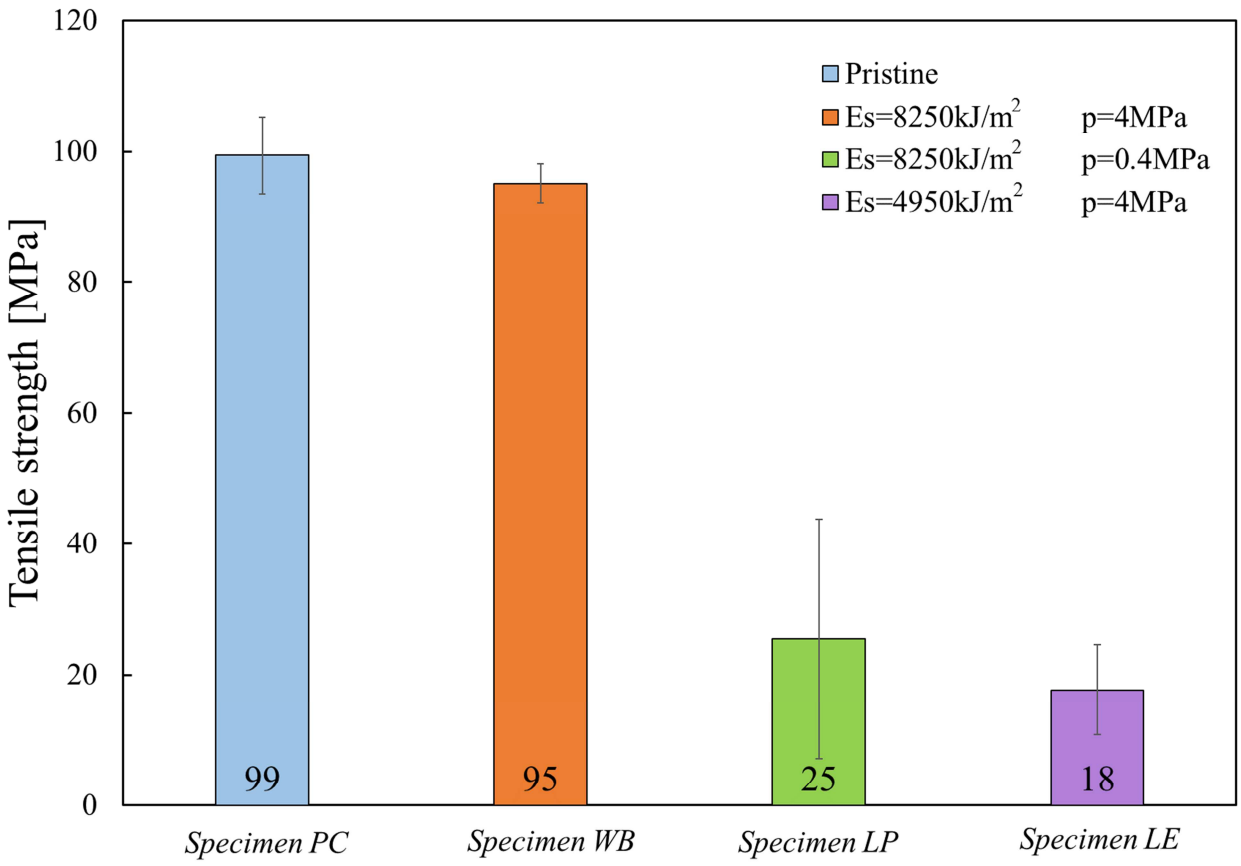

Figure 5 – Comparison between the tensile strength of pristine and welded samples. The error bars indicate the standard deviation.

The fracture surfaces of the *WB* and *PC* samples (Fig. 6a) show similar morphology being that of a cohesive fracture and indicating that effective molecular diffusion was achieved for the weld. In contrast, an adhesive type of fracture due to the insufficient pressure (*LP*) or input energy (*LE*) is seen for these specimens (Fig. 6c, d). The *LP* specimen (Fig. 6c) exhibits bubbling at the surface due to the inability of the applied pressure to overcome the high melt viscosity of the PEEK in order to expel entrained air or adsorbed moisture, whilst the *LE* specimen also shows partially unmelted material at the centre region because of insufficient heating time [6].

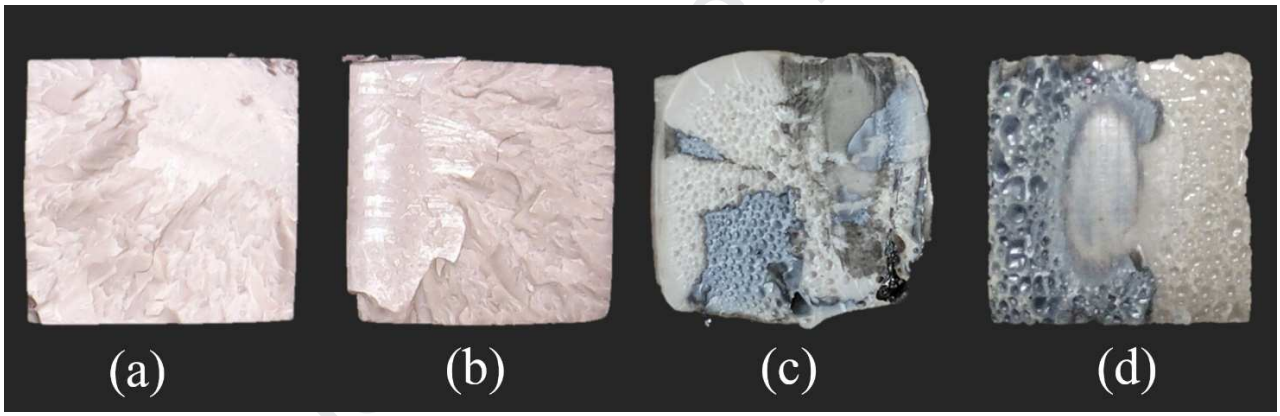

Figure 6 – Fracture surface of specimens after tensile test; (a) specimen PC; (b) specimen WB; (c) specimen LP; (d) specimen LE.

Conclusions

An innovative resistance welding method for thermoplastics, using CNT web as the directly energised Joule heating element, has been demonstrated. This preliminary investigation using PEEK specimens showed that the best results for bond tensile strength were achieved with a specific power of $W_s = 55$ kW/m^2, the specific energy of $E_s = 8250$ kJ/m^2, and a consolidation

pressure of $p = 4$ MPa. The welded specimens achieved a strength of 95 ± 3 MPa and a joint efficiency of 96%.

This proposed welding technology is anticipated to have a substantial impact. The manufacture of the CNT web is well understood and the method is scalable. The resulting small added weight and thickness, high conformability, and tailorable electro-thermal response make this approach highly practical for the welding of thermoplastic structures. It is envisaged that this may result in simpler, faster, and more reliable welding processes.

Acknowledgements

The authors gratefully acknowledge the financial support of the project SPaRK. SPaRK has received funding from the European Union's Horizon 2020 research and innovation programme under the Marie Sklodowska-Curie grant agreement No 754507. The authors would also like to acknowledge the financial support from the EPSRC project MACANTA—Multifunctional hierarchical advanced composite aerostructures utilising the combined properties of different carbon nanotube (CNT) assemblies (EP/N007190/1).

References

[1] Ageorges C, Ye L, Hou M. Advances in fusion bonding techniques for joining thermoplastic matrix composites: a review. Compos Part A Appl Sci Manuf 2001;32:839–57. doi:10.1016/S1359-835X(00)00166-4.

[2] Ageorges C, Ye L. Resistance Welding of Metal/Thermoplastic Composite Joints. J Thermoplast Compos Mater 2001;14:449–75. doi:10.1106/PN74-QXKH-7XBE-XKF5.

[3] Ageorges C, Ye L, Hou M. Experimental investigation of the resistance welding for thermoplastic-matrix composites. Part I: heating element and heat transfer. Compos Sci Technol 2000;60:1027–39. doi:10.1016/S0266-3538(00)00005-1.

[4] Ahmed TJ, Stavrov D, Bersee HEN, Beukers A. Induction welding of thermoplastic composites—an overview. Compos Part A Appl Sci Manuf 2006;37:1638–51. doi:10.1016/j.compositesa.2005.10.009.

[5] Bayerl T, Duhovic M, Mitschang P, Bhattacharyya D. The heating of polymer composites by electromagnetic induction – A review. Compos Part A Appl Sci Manuf 2014;57:27–40. doi:10.1016/j.compositesa.2013.10.024.

[6] Stavrov D, Bersee HEN. Resistance welding of thermoplastic composites-an overview. Compos Part A Appl Sci Manuf 2005;36:39–54. doi:10.1016/S1359-835X(04)00182-4.

[7] Yousefpour A, Hojjati M, Immarigeon JP. Fusion bonding/welding of thermoplastic composites. J Thermoplast Compos Mater 2004;17:303–41. doi:10.1177/0892705704045187.

[8] Ageorges C. Experimental investigation of the resistance welding of thermoplastic-matrix composites. Part II: optimum processing window and mechanical performance. Compos Sci Technol 2000;60:1191–202. doi:10.1016/S0266-3538(00)00025-7.

[9] Eveno EC, Gillespie JW. Resistance Welding of Graphite Polyetheretherketone Composites: An Experimental Investigation. J Thermoplast Compos Mater 1988. doi:10.1177/089270578800100402.

[10] Dubé M, Hubert P, Yousefpour A, Denault J. Resistance welding of thermoplastic composites skin/stringer joints. Compos Part A Appl Sci Manuf 2007;38:2541–52. doi:10.1016/j.compositesa.2007.07.014.

[11] Dubé M, Hubert P, Gallet JN, Stavrov D, Bersee HE, Yousefpour A. Metal mesh heating element size effect in resistance welding of thermoplastic composites. J Compos Mater 2012;46:911–9. doi:10.1177/0021998311412986.

[12] McKnight SH, Holmes ST, Gillespie JW, Lambing CLT, Marinelli JM. Scaling issues in resistance-welded thermoplastic composite joints. Adv Polym Technol 1997;16:279–95. doi:10.1002/(SICI)1098-2329(199711)16:4<279::AID-ADV3>3.0.CO;2-S.

[13] Brassard D, Dubé M, Tavares JR. Resistance welding of thermoplastic composites with a nanocomposite heating element. Compos Part B Eng 2019;165:779–84. doi:10.1016/j.compositesb.2019.02.038.

[14] Falzon BG, Catalanotti G, Hawkins SC, Russello M. Method and Apparatus for Joining Plastic Parts. Application No. GB1910505.5, Patent Pending, 2019.

[15] Yao X, Falzon BG, Hawkins SC. Orthotropic electro-thermal behaviour of highly-aligned carbon nanotube web based composites. Compos Sci Technol 2019;170:157–64. doi:10.1016/j.compscitech.2018.11.042.

[16] Yao X, Hawkins SC, Falzon BG. An advanced anti-icing/de-icing system utilizing highly aligned carbon nanotube webs. Carbon N Y 2018;136:130–8. doi:10.1016/j.carbon.2018.04.039.

[17] Hawkins SC, Poole JM, Huynh CP. Catalyst Distribution and Carbon Nanotube Morphology in Multilayer Forests by Mixed CVD Processes n.d. doi:10.1021/jp810072j.

Declaration of interests

☒ The authors declare that they have no known competing financial interests or personal relationships that could have appeared to influence the work reported in this paper.

☐The authors declare the following financial interests/personal relationships which may be considered as potential competing interests:

Highlights

- We have made an insert placing layers of CNT web between two PEEK films.
- We have embedded the CNT-web/PEEK inserts between two bonding surfaces.
- We have applied electrical current and pressure causing the welding of the parts.
- We have tested the welded joints in tension finding a joint efficiency of 96%.